scientific reports

Check for updates

OPEN

Menstrual blood serum extracellular vesicles reveal novel molecular biomarkers and potential endotypes of unexplained infertility

Kieran Brennan[1,2,7], Raminta Vaiciuleviciute[3,7], Ilona Uzieliene[3], Jolita Pachaleva[3], Zaneta Kasilovskiene[4], Lina Piesiniene[5], Eiva Bernotiene[3,6] & Margaret M. Mc Gee[1,2]✉

Several biomolecules have been previously associated with unexplained infertility (uIF) in blood and uterine samples, immune cells and their secreted factors, endometrial tissue, menstrual blood, serum, and stromal cells, however they do not comprehensively represent different uIF endotypes and their isolation/detection involves invasive diagnostic methods and lacks precision. This ex-vivo study was performed on extracellular vesicles (EVs) from menstrual blood collected on cycle day 2 from 9 fertile volunteers and 8 women with uIF. Menstrual blood serum (MBS) EVs were isolated from fertile and uIF MBS using Iodixanol Density Gradient Centrifugation and quantified by flow cytometry. EVs were characterized according to MISEV2023 guidelines. Comprehensive proteomic analysis of MBS EVs and EV-depleted MBS showed significant changes in uIF proteome, mostly affecting cell adhesion, immune response, apoptosis, response to oxidative stress and lipid metabolism. These processes were previously linked to pathologies of the female reproductive system but never investigated in uIF and were used to stratify patients into distinct molecular endotypes. Area under the curve (AUC) analysis was used to determine the optimum set of biomarkers for each of the uIF molecular endotypes. These findings provide new insights into uIF that could facilitate personalised treatment approaches.

Keywords Unexplained infertility, Menstrual blood serum, Molecular endotypes, Extracellular vesicles, Proteomics

Unexplained infertility (uIF) is a multifactorial condition affecting approximately 6% of the population worldwide[1,2]. The pathogenesis of uIF is not well understood although published studies show that a number of pathological processes, such as infection, oxidative stress, endometriosis and hormone alterations are involved in the development of uIF[3–8]. In most cases, improved diagnostic approaches would contribute to a better understanding of uIF and reveal new treatment options. Mechanistic pathways or endotypes were successfully applied for a few other diseases, such as asthma, to implement personalised therapy and reach better treatment outcomes[9]. However, there are currently no endotype-specific molecular biomarkers of uIF. Existing diagnostic methods of female reproductive diseases involve minimally invasive collection of peripheral blood and uterine flushing and more invasive approaches for the collection of follicular fluid or tissue biopsy[5,10–12].

During the past decade menstrual blood has received growing attention as a diagnostic approach that is non-invasive, ethically acceptable, and contains unique proteins and stem/progenitor cells that reflect the endometrial environment. It is easily accessible for self-collection and collection can be standardized to cycle day to avoid variations in protein levels caused by cyclical hormonal changes. Menstrual blood has already been presented as a non-invasively collected tissue for measurement of common biomarkers, such as cholesterol, cortisol, creatinine, high-sensitivity C-reactive protein, low density lipoproteins, Luteinizing Hormone, or triglycerides,

[1]School of Biomolecular and Biomedical Science, University College Dublin, Belfield, Dublin 4, Ireland. [2]Conway Institute of Biomolecular and Biomedical Research, University College Dublin, Belfield, Dublin 4, Ireland. [3] Department of Regenerative Medicine, Innovative Medicine Centre, Santariskiu str 5, LT-08406 Vilnius, Lithuania. [4]Medical Center "MAXMEDA", Vilnius, Lithuania. [5]Nanodiagnostika, Ltd., Vilnius, Lithuania. [6]Faculty of Fundamental Sciences, VilniusTech, Sauletekio al. 11, LT-10223 Vilnius, Lithuania. [7]Kieran Brennan and Raminta Vaiciuleviciute contributed equally to this work. ✉email: margaret.mcgee@ucd.ie

high density lipoproteins, glycated haemoglobin (HbA1c), Iron, Total T, Vitamin A and Vitamin D with no significant differences compared to peripheral blood serum values[13].

Menstrual blood consists of 3 main components: blood, vaginal fluid with mucus, and cells and fluid from shedding late secretory phase endometrial tissue with each component bringing its own proteome to menstrual blood samples[14,15]. Protein composition of vaginal fluid corresponds to proteins that are normally found in plasma, together with proteins of cell origin, mostly neutrophils[16]. Endometrial mesenchymal stromal cells and endothelial cells are found in menstrual blood together with a unique composition of immune cells. Menstrual blood has lower levels of lymphocytes and its subset T cells than peripheral blood, although levels of CD8+, Treg cells and NKT, uterine type NK cells are reported to be higher than in peripheral blood[17–20]. Cytokine analysis revealed that levels of complement component 5 (C5/C5a), granzyme A and B, interleukin-6 (IL-6), IL-1β, and CXCL8 were higher and IL-2, IL-12p70, XCL1/lymphotactin, and interferon-γ lower in menstrual blood plasma compared to peripheral blood plasma[21]. Furthermore, hormone levels in peripheral blood do not always correlate with levels in menstrual blood. For example, while hormones HbA1c, thyroid stimulating hormone (TSH), follicle-stimulating hormone (FSH), anti-müllerian hormone (AMH), and LH in menstrual blood are highly correlated with venipuncture samples[22], prolactin and LH levels were higher in menstrual plasma than in peripheral blood, whereas estradiol was slightly lower and FSH with progesterone levels were significantly lower than peripheral level making menstrual blood a preferable source for infertility biomarkers[23,24]. Menstrual blood was already used for diagnosis of female reproductive tract diseases, such as endometriosis, gynecological cancer, human papillomavirus (HPV)[25–27]. Collectively these studies demonstrate that menstrual blood is a valuable biofluid for diagnosis of various health conditions in females, whereas for reproductive diseases, it may hold strong advantage due to representation of local events in the reproductive system. However, it was never used for the investigation of uIF endotypes.

Extracellular vesicles (EVs) are found in all human fluids and tissues and contain cargo including proteins, metabolites, nucleic acids. There is a growing interest in EVs as a source of diagnostic biomarkers, with the majority of studies focusing on cancer and cardiovascular disease[28]. There are attempts to analyse EVs from uterine fluid or endometrial cells in the human reproductive system as a diagnostic or treatment approach, although the majority of studies to date have been performed in animals.

EVs are reported to regulate early embryo development by facilitating embryo-endometrium communication, through the selective packaging of proteins and nucleic acids, which are protected from extracellular degradation within the lipid bilayer of the vesicle. It has been shown that trophoblast derived EVs induced transcriptomic changes in the RL 95–2 endometrial cells[29,30]. Rai, et al. reported that the uterine lavage EV proteome changes substantially during distinct phases of the natural menstrual cycle, and between fertile and infertile women, with both antioxidant and invasive proteins being delivered to trophectoderm cells following EV uptake[31]. The importance of antioxidant activity is supported by increased implantation rates and ongoing pregnancy rates during in vitro fertilization (IVF) and embryo culture when using media with three antioxidants Acetyl-L-Carnitine (ALC), N-Acetyl-L-Cysteine (NAC) and a-Lipoic Acid (ALA)[32]. Furthermore, mouse embryos treated with EVs secreted from endometrial cells from women with recurrent implantation failure had reduced blastocyst cell numbers and a decreased embryonic invasion capacity compared to EVs from fertile women[32]. In addition, endometrial EVs have been shown to enhance human trophectoderm spheroid adhesion to the and invasion capacity endometrial epithelium[33,34].

The endometrial EV proteome is affected by hormone changes, with oestrogen and progesterone treatment (mimicking the receptive phase) increasing the levels of several proteins identified in various embryo implantation models (CDH5, HSPG2, KIF5C and EIF4E), and endometrial receptivity models (PLAT, ACE2, and INHBB) compared to both oestrogen (proliferative phase), or progesterone (secretory phase) treated endometrial cell derived EVs[35]. The endometrial EV function also appears to change after implantation with pre-implantation uterine fluid EVs up-regulating the expression of apoptosis-related genes in primary bovine endometrial epithelial cells, while post-implantation uterine fluid EVs up-regulated the expression of adhesion molecules[36].

Uterine fluid EVs may also promote fertility by preserving sperm function and sperm survival within the female genital tract[37]. Oviductal EVs improved cat sperm motility, and the fertilizing capacity of cat spermatozoa and prevented acrosomal exocytosis in vitro[38], while increasing sperm survival and reducing sperm motility in pigs[39]. A potential mechanism is the EV-mediated delivery of protein cargo to sperm, with murine vaginal EVs being shown to be capable of delivering SPAM1, PMCA1/4, and PMCA1 to sperm[40]. Furthermore, uptake of oviductal EVs by murine sperm resulted in up to a ~ 3-fold increase of plasma membrane Ca^{2+}-ATPase 4a (PMCA4a) in the sperm[41] and Pmca4 deletion leads to loss of sperm motility and male infertility[42].

The EV cargo has been reported to change in response to diseases such as endometriosis and polycystic ovary syndrome, with 5 proteins, PRDX1, histone H2A type 2-C, ANXA2, ITIH4 (fragment), and tubulin α-chain found exclusively in peritoneal fluid EVs from endometriosis patients relative to healthy controls[43]. S100-A9 protein is higher in the EVs derived from follicular fluid of polycystic ovary syndrome patients. S100-A9 + EVs from human follicular fluid significantly enhanced inflammation and disrupted steroidogenesis via activation of nuclear factor kappa B (NF-κB) signalling pathway.

Isolation of EVs from menstrual blood serum (MBS) has not been reported before although it can bring valuable information about alterations in the endometrium that may be associated with female infertility pathogenesis. In this study MBS was collected from fertile females and females with uIF and MBS EVs were isolated by density gradient ultracentrifugation and compared with the EV-depleted supernatant. Proteomic characterisation of the MBS EVs and EV-depleted supernatant samples has revealed significantly dysregulated cargo in MBS EVs from females with uIF and the identification of novel molecular endotypes of uIF. Overall this study provides new insights into uIF that could facilitate personalised treatment approaches.

Results

EVs isolation and characterization from menstrual blood serum (MBS)

EVs were successfully isolated from the MBS of fertile females and females with uIF, using Iodixanol Density Gradient Centrifugation, and their characterisation was performed according to the MISEV2023 guidelines[44]. MBS EV isolation was confirmed by visualisation using TEM (Fig. 1A). Western blot analysis showed the presence of intravesicular EV marker TSG101 and transmembrane marker CD63, and a significant reduction in the abundance of albumin and apolipoproteins APOA1, APOB and APOE compared to MBS samples (Fig. 1B). EV quantification showed significantly higher amounts of EVs detected in MBS samples obtained from infertile females relative to fertile (Fig. 1C). The detected EVs were 180–4000 nm (approximate EV sizes were attributed to the 80–500 nm PS beads based on Rosetta calibration), with no difference in EV size from fertile and infertile female samples (data not shown). Flow cytometry analysis confirmed the presence of transmembrane proteins CD9, CD63, CD81, and CD147, with no differences in protein expression levels in MBS EVs from fertile and infertile females (Fig. 1D).

These results demonstrate for the first time the successful isolation and characterisation of EVs from fertile and infertile female MBS according to the MISEV2023 guidelines.

Proteome profiling of menstrual blood serum (MBS) and EV-depleted MBS

To detect potential biomarkers of uIF, EV cargo was analysed by mass spectrometry and proteomic profiles obtained for MBS EVs and EV-depleted MBS sample groups were compared between fertile and infertile groups.

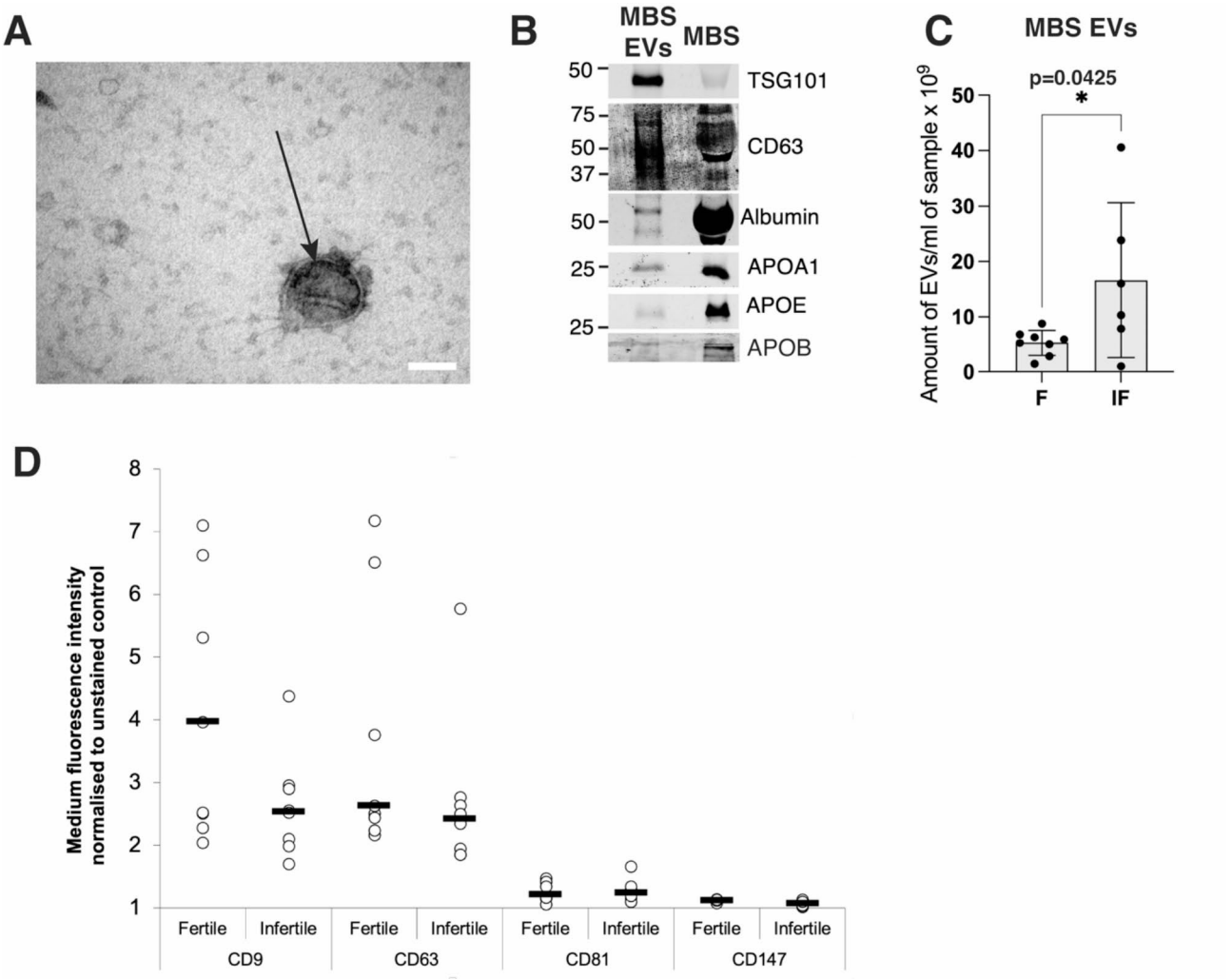

Fig. 1. Confirmation of MBS EVs (**A**) Representative negative staining TEM image of MBS EVs. Scale bar = 100 nm. Arrows indicate EV. (**B**) Western blot comparing MBS EVs with the MBS they were isolated from, showing the level of enrichment of the EV markers; TSG101, CD63, while depleting the levels of the common contaminants; albumin, APOA1, APOB and APOE. (**C**) Amount of EVs normalised to initial sample volume of MBS from fertile (F) and infertile (IF) females. A statistically significant difference ($p < 0.05$) is indicated by an asterisk (*). (**D**) MBS EV transmembrane markers (CD9, CD63, CD81, CD147) expression analysis performed by flow cytometry.

First, proteomic analysis revealed that 87 and 90 proteins that are listed in the Vesiclepedia Top 100 proteins, were detected in MBS EVs of infertile females and fertile females respectively. Furthermore, 667 proteins were shared between fertile and infertile female MBS EVs (Fig. 2A). 1078 proteins were detected in MBS EVs and 656 proteins in EV-depleted MBS (Fig. 2B). In the fertile group, 261 proteins were detected in EV-depleted MBS, 690 in MBS EVs, and 368 proteins were detected in both sample types. In the infertile group, 283 proteins were detected in EV-depleted MBS, 463 in MBS EVs and 315 in both sample types (Fig. 2C).

Proteomic analysis revealed that MBS EVs from fertile and infertile groups had a higher number of proteins than EV-depleted MBS. Importantly our data revealed that MBS EVs from females with uIF had a lower number of proteins compared to fertile. The identification of differentially enriched proteins between fertile and infertile MBS EVs may reveal biomarkers of uIF and provide valuable insight into the disease pathogenesis.

Comparison of the proteome content of MBS EVs and EV-depleted MBS with the Human Protein Atlas project (HPA) revealed that proteins detected in MBS EVs and EV-depleted MBS from the two female groups have also been detected in a variety of cells present in human endometrium including glandular cells, cells in endometrial stroma, stromal fibroblasts, luminal and glandular epithelial cells, immune cells (macrophages, lymphocytes), endothelial cells, and ciliated epithelial cells (Supplemental Fig. S2).

Proteome analysis of EV-depleted menstrual blood serum (MBS) from fertile and infertile females

After observing differences in the number of proteins expressed in MBS EVs and EV-depleted MBS from fertile and infertile females, proteins that are significantly differentially enriched or reduced in each compartment during infertility were analysed further.

Proteomic analysis revealed a significant increase in 6 proteins and decrease in 15 proteins in EV-depleted MBS of infertile females compared to fertile females. Figure 3A shows a volcano plot of significantly enriched and reduced proteins in EV-depleted MBS from infertile females. A heatmap revealed significantly dysregulated protein in EV-depleted MBS from fertile and infertile females (Fig. 3B). Finally, 2D Principal Component Analysis (PCA) shows a partial overlap in the principal components of EV-depleted MBS from fertile and infertile females (Fig. 3C). Overall, these data reveal only a small number of dysregulated proteins in the EV-depleted MBS from females with uIF, whereas the majority of proteins detected were unchanged across F and IF groups.

Proteins downregulated in EV-depleted MBS from infertile females were also detected in HPA glandular cells and cells in endometrial stroma, stromal fibroblasts, smooth muscle cells, and endothelial cells, while proteins upregulated in infertile females were only detected in HPA glandular cells and cells in the endometrial stroma (Supplemental Fig. S3). Gene ontology analysis of upregulated proteins in infertile female EV-depleted MBS did not reveal any significantly changed biological processes or cellular components. However, serine-type endopeptidase inhibitor activity is upregulated in infertile females. In contrast, processes related to hypoxia response, lipid metabolism and embryo implantation are downregulated in EV-depleted MBS from infertile women. Calcium ion binding, lipid transporter activity, protein binding, and copper ion binding functions were reduced in infertile female EV-depleted MBS. Furthermore, reactome pathway analysis reported a reduction in extracellular matrix (ECM) organisation in EV-depleted MBS from infertile females.

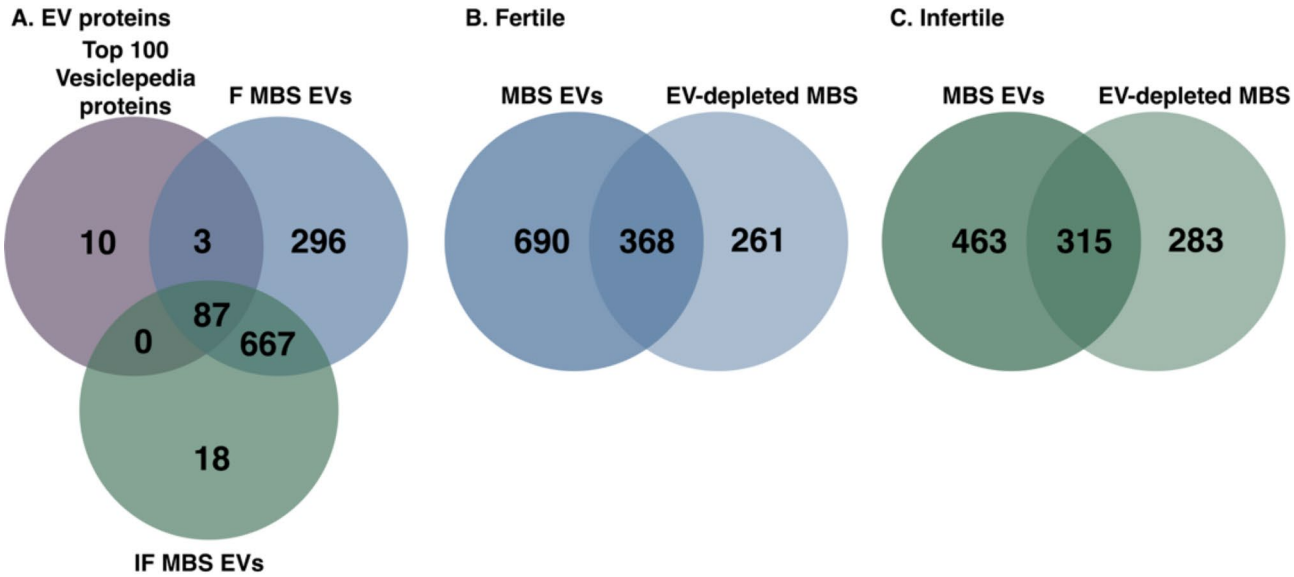

Fig. 2. Comparative analysis of protein number identified in MBS EVs and EV-depleted MBS by mass spectrometry. (**A**) Venn diagram of proteins detected in EVs from fertile and infertile female MBS compared to the Vesiclepedia Top 100 proteins, Total proteins detected in MBS EVs, and EV-depleted MBS from fertile (**B**) and infertile (**C**) females.

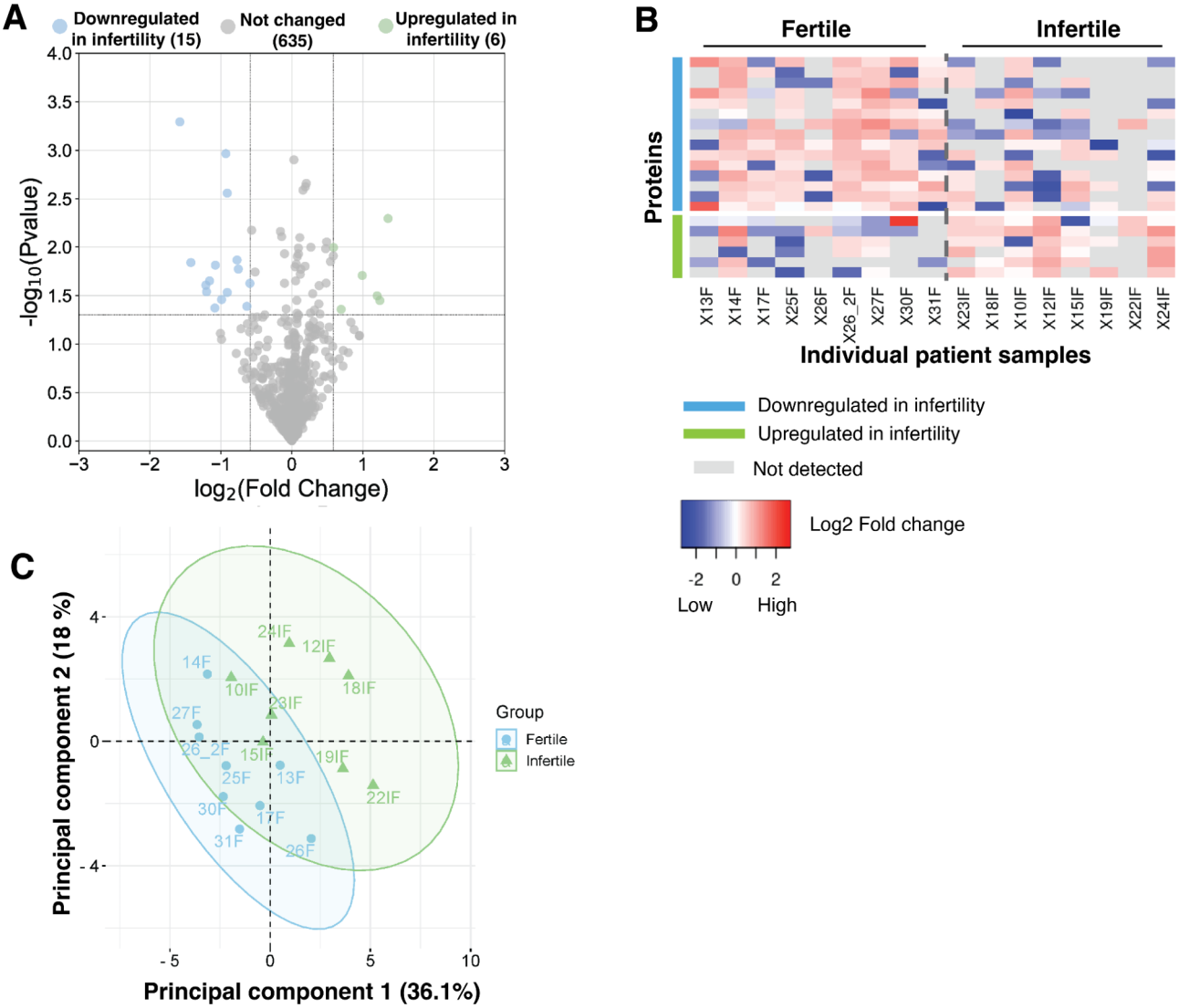

Fig. 3. Proteome analysis of EV-depleted MBS from fertile females and females with uIF. (**A**) Volcano plots of the differentially expressed proteins in EV-depleted MBS from infertile females samples compared to fertile. Adjusted p values (− log10) are plotted against the fold changes (log2). Blue dots represent reduced proteins and green dots represent enriched proteins in uIF group as compared to the fertile controls. (**B**) Heatmap of significantly altered proteins in EV-depleted MBS. The down-regulated and up-regulated proteins in infertile are ranked by log2 fold change, colour represents the abundance of significantly changed proteins (red: increased; blue: reduced). (**C**) Principal component (PC) analysis of proteins from fertile (blue) and infertile (green) groups. In each axis, the percentage represents the total variability between all points.

Proteome analysis of menstrual blood serum (MBS) EVs from fertile and infertile females

Comparison of differentially enriched proteins in the MBS EVs from fertile and infertile females revealed that 4 proteins were increased and 266 proteins were decreased in MBS EVs from infertile females, compared to fertile females. A volcano plot of significantly enriched and reduced proteins in MBS EVs from infertile females is presented in Fig. 4A. A heatmap revealed significantly dysregulated proteins in MBS EVs from fertile and infertile females (Fig. 4B). 2D Principal Component Analysis (PCA) showed that the principal components of MBS EVs from fertile and infertile females can be separated (Fig. 4C), however it is noted that the heatmap and PCA analysis revealed that MBS EVs from patient 23IF has a proteome profile similar to that of fertile MBS EVs. Overall this data demonstrates that the MBS EV proteome from fertile and infertile females are significantly different. Deeper analysis of dysregulated proteins may reveal biomarkers and uIF and provide mechanistic insight into the molecular mechanism involved.

Proteins that were found to be significantly differentially enriched in MBS EVs from infertile females were compared to proteins detected in different endometrial cells in the Human Protein Atlas project. (Supplemental Fig. S4). Downregulated proteins in infertility were found in all types of endometrial cells with the highest numbers in glandular cells and cells in endometrial stroma. Only one protein found in glandular cells was upregulated in infertility.

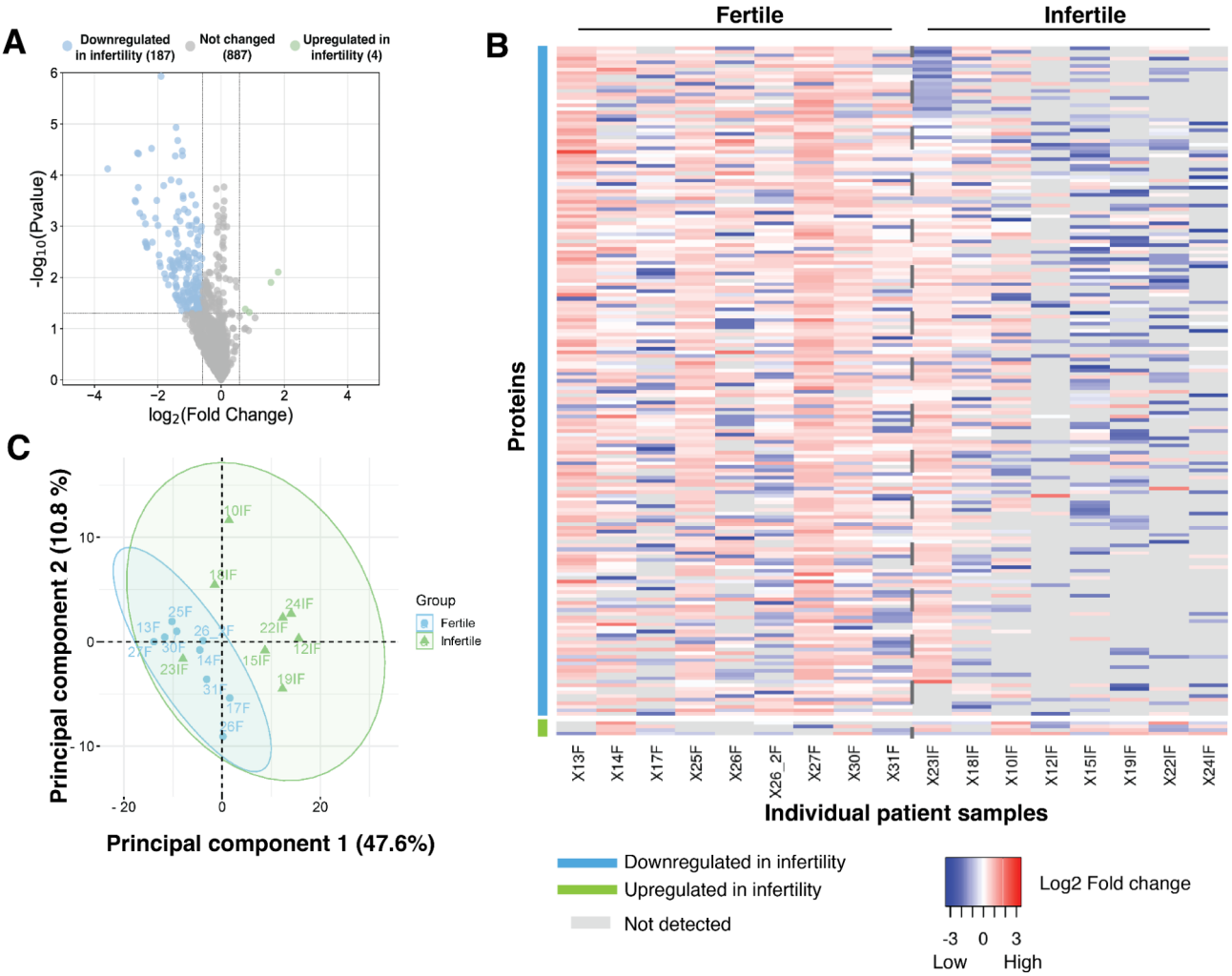

Fig. 4. Proteome analysis of MBS EVs from fertile females and females with uIF. (**A**) Volcano plots of the differentially expressed proteins in MBS EVs from infertile females samples compared to fertile. Adjusted p values (− log10) are plotted against the fold changes (log2). Blue dots represent reduced proteins and green dots represent enriched proteins in uIF group as compared to the fertile controls. (**B**) Heatmap of significantly altered proteins in MBS EVs. The up-regulated and down-regulated proteins in infertile are ranked by log2 fold change, colours represent the abundance of significantly changed proteins (red: increased; blue: reduced). (**C**) Principal component (PC) analysis of proteins from fertile (blue) and infertile (green) groups. In each axis, the percentage represents the total variability between all points.

Proteins that were downregulated in MBS EV from infertile patients were analysed using Markov Cluster Algorithm (MCA) using inflation parameter 2 to reveal 14 clusters containing 4 or more proteins. Proteins belonging to the most abundant clusters participate in proteolysis, signal transduction, cell division, endocytosis, RNA metabolic processes, cell adhesion, oxidative phosphorylation, cellular lipid metabolic processes, and positive regulation of immune response (Supplemental Table S1).

Gene ontology analysis revealed that the significantly downregulated proteins are associated with the regulation of proteolysis, leukotriene biosynthesis, apoptosis, vesicle-mediated transport, protein transport, and others (Fig. 5A). Furthermore, downregulated proteins in MBS EVs belong to the extracellular exosome, cytosol, and proteasome complex (Fig. 5B) and their associated functions include protein binding, cadherin binding, RNA binding, and enzyme activities including proteasome-activating ATPase, peptidase, and peroxidase (Fig. 5C).

Finally, reactome pathway analysis revealed that cell cycle and signal transduction-related pathways, immune signalling, programmed cell death and metabolism are downregulated in MBS EVs isolated from infertile females (Fig. 6).

Stratification of patients with unexplained infertility (uIF) into molecular endotypes

Five biological processes are proposed as unique endotypes of uIF based on the most significant results from GO, Reactome pathway, clustering data and literature review: cell adhesion, immune response, oxidative stress, lipid metabolism and apoptosis. To examine whether the uIF cohort consists of women with different causes of

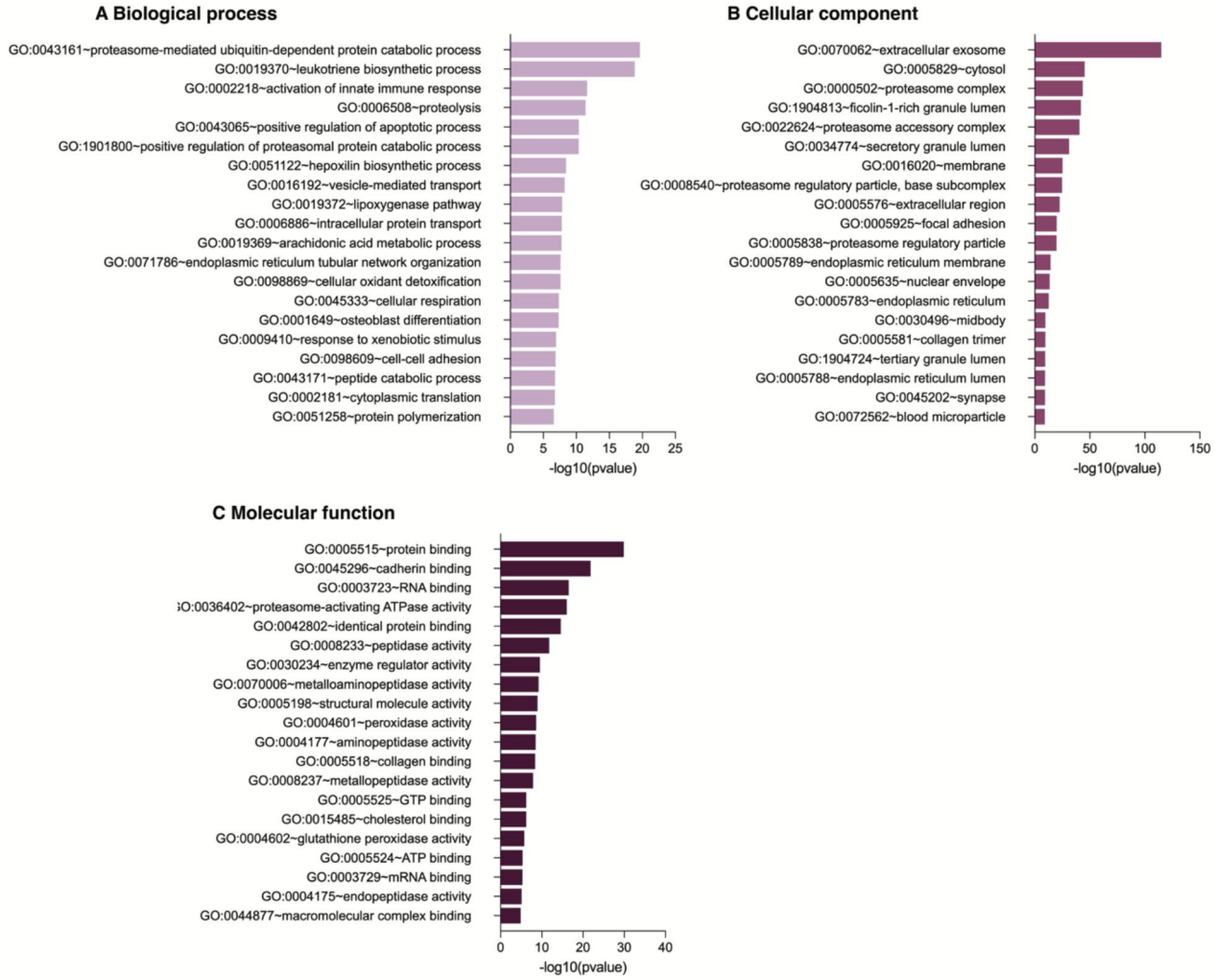

Fig. 5. Gene ontology analysis of downregulated proteins in MBS EVs from females with uIF. Biological processes (**A**), cellular components (**B**), molecular functions (**C**) of reduced MBS EVs proteins in infertility. Top 20 results are presented in the graphs, results are listed based on – log10 (p-value).

infertility we next analysed the proteome data on an individual level. For each endotype prediction overview analysis was performed to identify outliers that did not have alterations in these processes, such as 23IF which did not qualify for any endotype while 18IF qualified for only 2 endotypes (Supplemental Table S2). 23IF was a clear outlier for all endotypes thereby suggesting the existence of other unidentified mechanisms of uIF, such as ovarian health or other unidentified genetic factors.

Patient stratification was performed using MBS EV data. Females 18IF and 23IF samples were evaluated as outliers in the Altered immune response group and they were subsequently added to the Normal immune response IF group, while the remaining IF females were grouped as Altered immune response IF group (Fig. 7A). The level of SYK was significantly lower in the Altered immune response IF group compared to Normal immune response IF and F groups (Fig. 7B). Females 10IF, 18IF and 23IF samples were selected as outliers in the Altered response to oxidative stress group and they were added to the Normal response to oxidative stress IF group, while the remaining IF females were grouped as the Altered response to oxidative stress IF group (Fig. 7C). The level of MGST2 was significantly lower in the Altered response to oxidative stress IF group compared to the Normal response to oxidative stress IF and F groups (Fig. 7D). Female 18IF, 22IF, 23IF samples were selected as outliers in the Altered apoptosis group and they were added to the Normal apoptosis IF group, while the remaining IF females were grouped as Altered apoptosis IF group. (Fig. 7E). Levels of PSMC4, PSMC6, PSMD2, PSMD7 were significantly lower in the Altered apoptosis IF group compared to Normal apoptosis IF and F groups (Fig. 7F). Females 15IF, 23IF samples were selected as outliers in the Altered lipid metabolism group and they were added to the Normal lipid metabolism IF group, while the remaining IF females were grouped as Altered lipid metabolism IF group (Fig. 7G). Levels of FASN and MGLL were significantly lower in the Altered lipid metabolism IF group compared to Normal lipid metabolism IF and F groups (Fig. 7H). There was only one outlier (Female 23IF) in the Altered cell adhesion group making it the most uniform group, typical for most of the samples of uIF (Fig. 7I).

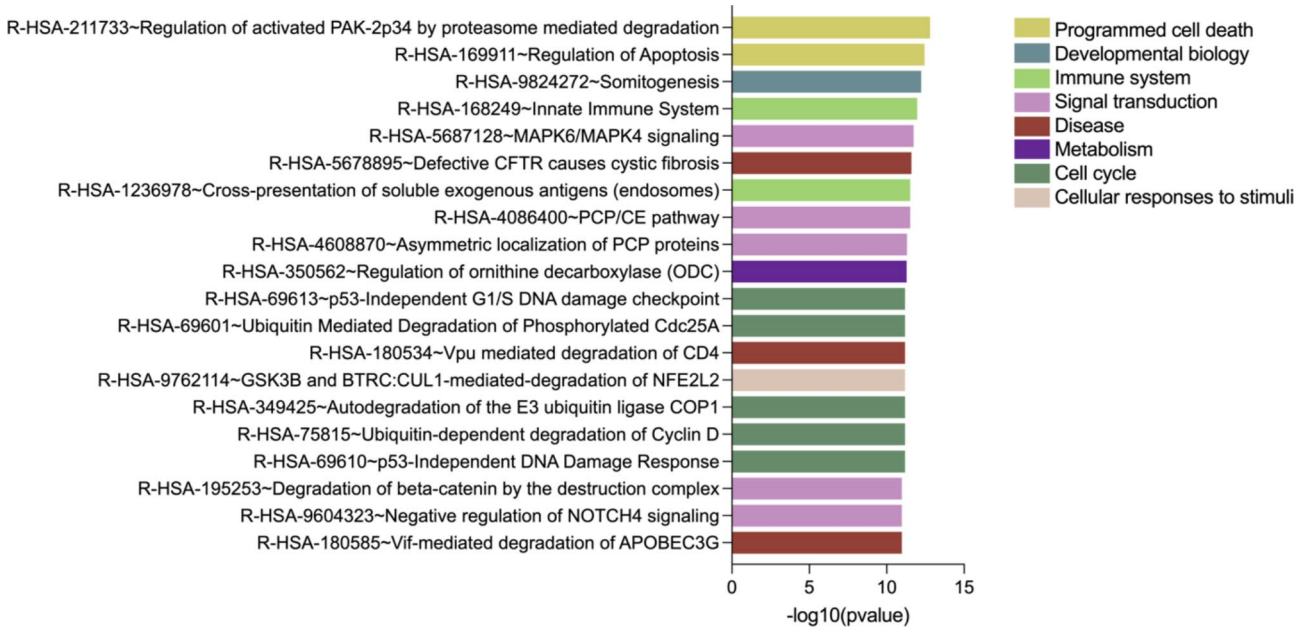

Fig. 6. Reactome pathway analysis of reduced proteins in MBS EVs of females with infertility. Top 20 results are presented in the graphs with – log10 (p-value), different pathways groups are presented in different colours.

This data shows that patients with uIF have different protein profiles and groups of endotypes should be analysed separately.

Identification of biomarkers for each molecular endotype of unexplained infertility (uIF)

After identifying molecular endotypes of uIF, analysis of their biomarkers, that could be used for diagnostic purposes, was performed. Biomarkers of each uIF molecular endotype were analysed by plotting AUC curves. All samples of the fertile group and only samples of uIF females with altered processes, were used for the analysis. Selected frequency analysis was performed (Supplemental Fig. S5) and results with the highest value were used for the AUC curve. For Altered cell adhesion endotype CTNNB1, COL6A1, MYH10, EMILIN1, CD226, ITGA3, ITGA1 HABP2, PXDN and TM9SF3 proteins were selected and their combination resulted in AUC value of 0.999 confirming this combination of adhesion proteins is specific and sensitive for detecting altered cell adhesion (Fig. 8A). For Altered lipid metabolism a combination of FASN, MGLL, CYC1, CPT1A, COX4I1 gave AUC value of 0.915 (Fig. 8B). The AUC value of Altered immune response proteins SYK, C1QC, PGLYRP2, TBK1, DDX3X, ENDOD1, CHID1, PRKDC is 0.985 (Fig. 8C). Altered response to oxidative stress proteins PSMB5, GPX8, GPX4, ERO1L resulted in AUC 0.951 (Fig. 8D) and a combination of Altered apoptosis proteins PSMD2, PSMB5 and MAPK1 had AUC = 1 (Fig. 8E).

Discussion

Women who are unable to conceive after 1 year, when there is no diagnosable reason for infertility, will receive a diagnosis of unexplained infertility (uIF). The current diagnostic methods lack the precision necessary to determine if these women have the same etiopathogenetic mechanism or whether this diagnosis comprises multiple female health conditions presenting with the similar outcome. Recent studies have demonstrated correlations between uIF and conditions such as endometriosis, infectious diseases, and hormonal changes, however a root cause remains unknown[3–8]. New diagnostic biomarkers are needed to improve monitoring of women with uIF in order to gain a mechanistic understanding of molecular pathways of the condition development and to more precisely identify potential asymptomatic causes of infertility such as inflammation, abnormal cell adhesion in endometrium or etc. In addition to improved diagnosis, new prognostic markers may one day identify whether some women would benefit from lifestyle changes or some general therapy, while other women would need one or more targeted treatments including ovulation induction, intrauterine insemination (IUI), or IVF.

This study focuses on menstrual blood serum (MBS) as a potential source of biomarkers, as MBS has many advantages for routine monitoring of women with uIF. MBS has the potential for non-invasive self-collection and MBS biomarker screening has the ability to reflect the endometrial environment in a way that can be standardized to cycle day thereby reducing the influence of cyclical hormonal changes. In the past decade menstrual blood has received growing attention as a source of biomarkers and is already used for diagnosis of female reproductive tract diseases, such as endometriosis, gynaecological cancer, HPV infection. In this study we focused on two aspects of MBS, the MBS EVs and the EV-depleted MBS. MBS EVs were characterised in accordance with the MISEV2023 guidelines and it was observed that women with uIF had significantly more EVs while there was no significant change in EV size. In the cargo of these EVs no difference in the abundance of EV markers on the EVs

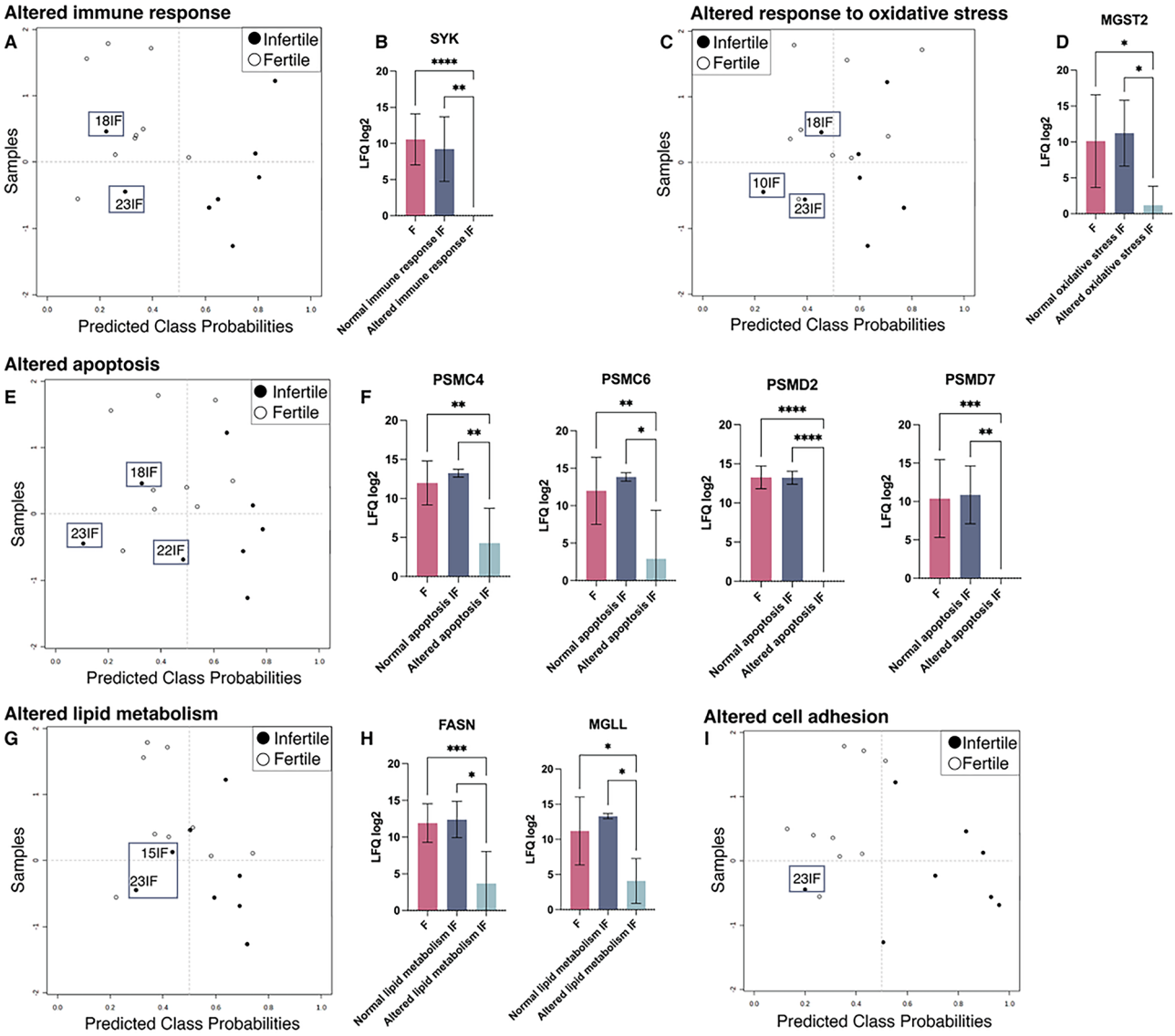

Fig. 7. Identification of molecular endotypes of uIF. Outliers were identified using Metaboanalyst 4.0 (accessed on 16 August 2024): (**A**, **B**) Altered immune response, (**C**, **D**) Altered response to oxidative stress, (**E**, **F**) Altered apoptosis, (**G**, **H**) Altered lipid metabolism and (**I**) Altered cell adhesion in MBS EVs samples. (**A**, **C**, **E**, **G**, **I**) Prediction overview analysis with identification of outliers and (**B**, **D**, **F**, **H**) significant proteins between normal and altered IF groups are presented, $^{*}p < 0.05$, $^{**}p < 0.01$, $^{***}p < 0.001$.

was determined, while proteomic analysis revealed a greater number of proteins with reduced levels rather than increased in uIF samples. This pattern was replicated in the EV-depleted MBS samples.

Since the altered protein levels in the MBS EVs and the EV-depleted MBS could be originating from multiple cell sources, the proteomic data was compared with the Human Protein Atlas project data to gain information on the cell types affected during uIF. The proteins decreased in uIF MBS EVs were associated with all types of endometrial cells, while proteins decreased in uIF EV-depleted MBS were associated with glandular cells, endometrial stroma, fibroblasts smooth muscle and endothelial cells, but not with epithelial cells, lymphocytes or macrophages. The proteins increased in uIF MBS EVs were associated with only glandular cells and endometrial stroma, while proteins increased in uIF EV-depleted MBS were only associated with glandular cells. Overall it was found that altered MBS EV protein cargo provides important information on altered molecular pathways in uIF. These pathways include cell adhesion, proteolysis, leukotriene biosynthetic process, apoptosis regulation, vesicle mediated transport, protein transport and others which are related to endometriosis, implantation failure, impaired decidualization[45–47] while in EV-depleted MBS only serine-type endopeptidase inhibitor activity, response to hypoxia, lipid metabolism proteins and embryo implantation was altered. This shows that MBS EVs can provide more information on altered pathways in uIF. Personalised analysis of the proteomic data helped to individually identify altered processes in each patient. These processes were grouped into several endotypes,

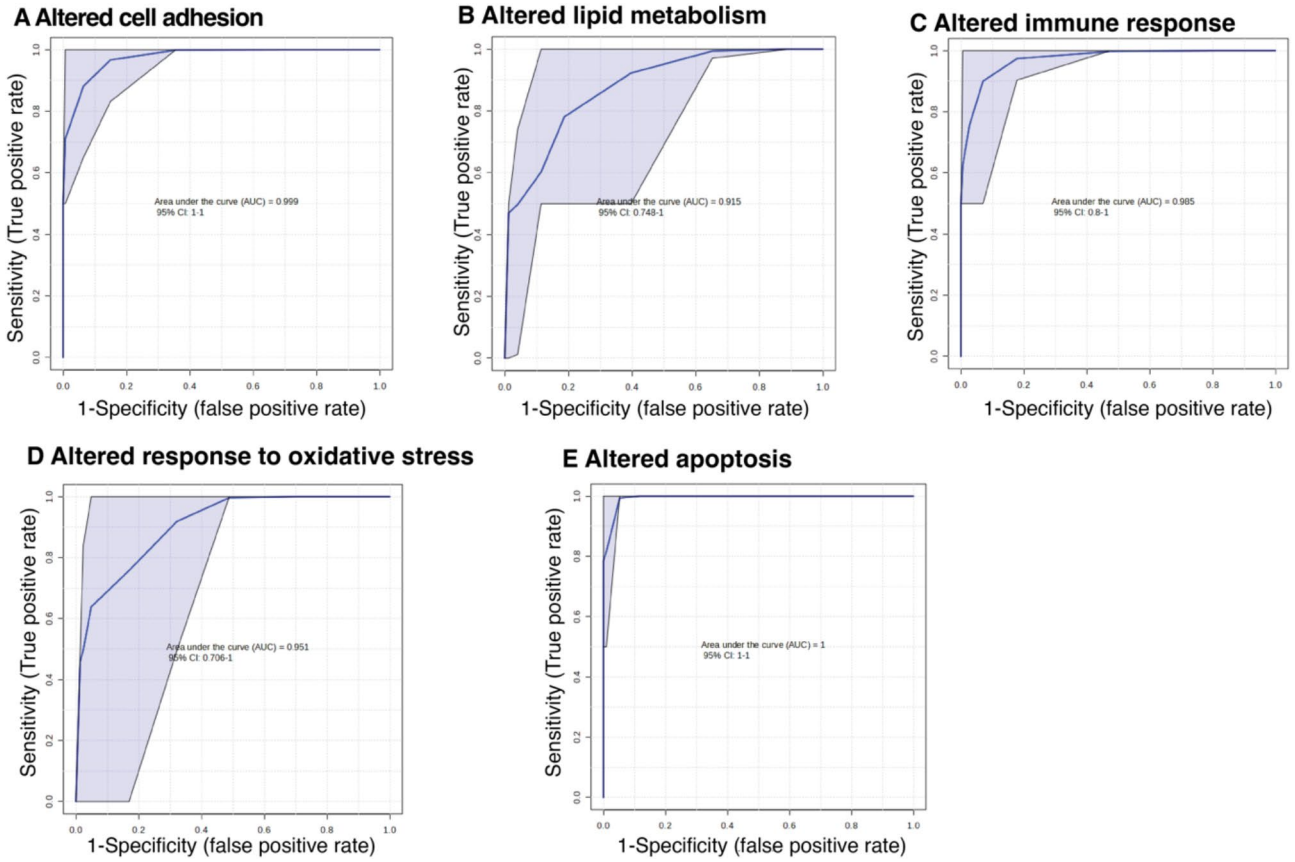

Fig. 8. Performance of uIF biomarker panel based on MBS EV proteome profiling. ROC curves and their 95% CI on the discovery set are shown in blue. (**A**) Altered cell adhesion, (**B**) Altered lipid metabolism, (**C**) Altered immune response, (**D**) Altered response to oxidative stress, (**E**) Altered apoptosis.

including cell adhesion, immune response, proteolysis, lipid metabolism and response to oxidative stress, as all these processes may appear closely related to pathogenesis of infertility (Supplemental Table S3).

Stratification of uIF patients into potential endotypes revealed that the majority of women with uIF have a combination of several endotypes although there are patients, such as 23IF which qualify for none of the suggested endotypes while 18IF qualified for only 2 of the endotypes (Supplemental Table S2). Following assignment to these uIF endotypes, area under the curve (AUC) analysis was used to determine the optimum set of biomarkers of each uIF molecular endotype from the MBS EV proteomic data. A 10-protein panel resulted in AUC value of 0.999 for the cell adhesion endotype, while an 8-protein panel resulted in AUC value of 0.985 for the immune response endotype. The lipid metabolism endotype had an AUC value of 0.915 with a 5-protein panel, the oxidative stress endotype had an AUC value of 0.951 with a 4-protein panel, and the apoptosis endotype had an AUC value of 1 with a 3-protein panel of PSMD2, PSMB5 and MAPK1. Several of these proteins have already been linked with infertility or related processes (Supplemental Table S3), however, further studies involving a larger number of women are needed to determine the validity of these markers for personalised approach. Altered cell adhesion was the main molecular endotype that was detected in the vast majority of samples of females with uIF, and this might imply the issues related to embryo implantation.

In this study we separated MBS into MBS EVs and EV-depleted MBS and observed differences in the proteins and related processes associated with uIF in the two fractions. It should be highlighted that while albumin was greatly reduced in the MBS EV preparations, it was not completely removed. The capture of soluble proteins such as albumin is a limitation of all human plasma EV studies, this is evident by albumin reported as the 25th most abundant EV protein according to Vesiclepedia[48]. It is also possible that albumin and other soluble proteins are present as part of the EV corona as reported[49], rather than specific EV proteins. These are important considerations for future validation of biomarkers identified in this study, as different EV isolation methods will impact the EV corona in different ways. Further studies are also needed to validate the results of this study in a larger cohort torepresent a broader population of women with uIF.

This study highlights the potential of MBS EVs as a source of biomarkers of uIF molecular endotypes. Moreover, stratification of women according to endotypes could guide personalised treatment options. For instance, laparoscopy could be used to further diagnose asymptomatic endometriosis in inflammatory endotype, whereas progesterone-induced blocking factor (PIBF) and IL-4 immunomodulators may be proposed for the treatment of an altered immune response. Antioxidant treatment may be applicable for females with altered response to oxidative stress as it has been shown that antioxidants reduce pain and inflammation in patients

with endometriosis[50]. Patients with altered adhesion could benefit from estrogen and progesterone treatment which increases production of endometrial extracellular matrix[51]. Furthermore, the prognostic potential of the endotype panels could contribute to the prediction of IVF or conservative personalised treatment need, and in turn, their success rates, and thereby become a useful decision making tool for uIF management. Further studies with larger cohorts and longitudinal sampling are required to follow the course of disease and determine responses to potential personalised targeted treatments, seeking to achieve the maximum clinical benefit of these endotype panels.

Taken together, the findings of this study demonstrate that MBS EVs carry molecular cargo with potential to identify specific mechanistic molecular endotypes of unexplained infertility: altered cell adhesion, lipid metabolism, immune response, apoptosis and response to oxidative stress.

Materials and methods

Menstrual blood collection from fertile and infertile females

Menstrual blood was collected from 17 female donors: 9 fertile (F) and 8 with unexplained infertility (uIF) following informed consent from the MaxMeda gynecological clinic (Vilnius, Lithuania) and/or directly delivered (anonymously) to Santariškių st. 5, State Research Institute Innovative Medicine Centre (IMC), according to the valid bioethics permission 2014-06-10 No. 158200-14-741-257 and its addition, No. 158200-741-PP2-34. All participants provided written informed consent prior to enrolment in the study. Volunteers were selected according to the following criteria: age category (24–40 years), normal body mass index (BMI), regular menstrual cycle length (25–31 days), absence of concomitant diseases (including gynecological, immune, hormonal disorders and other acute and chronic diseases). Fertile donors were selected based on the presence of children (at least one child) and infertile females included those unable to conceive for at least one year, without cycle changes, not using contraceptive drugs and having fertile partners. 1–20 ml of menstrual blood was centrifuged at 400 × g for 40 min using Ficoll-Paque PLUS (Cytiva, Sweden) density gradient centrifugation. MBS was collected from the top layer and frozen at -80 °C. All aspects of this study, including research methods and obtaining informed consent, were conducted in strict accordance with regulations of the Vilnius Regional Committee for Biomedical Research Ethics.

EV isolation from menstrual blood serum (MBS) by iodixanol density gradient centrifugation

EVs were isolated from 2 to 10 ml MBS based on previously described methods[52].

All ultracentrifugations were performed in Beckman Coulter rotors (Beckman Coulter, USA) and ultracentrifuge tubes at 120,000 g AVG in Beckman Coulter Optima L-100 XP or Beckman Coulter Optima MAX-XP ultracentrifuges (Beckman Coulter, USA), with centrifugation durations based on a "50 nm cut-off size" adjustment to the centrifugation duration for each rotor as described in Livshits et al. 2015, with additional 5 min added to allow the rotor to come up to speed[53].

MBS samples were defrosted and diluted with particle-free Phosphate-buffered saline (PBS; Sigma Aldrich, USA) before centrifugation twice at 2500 × g for 15 min in an SX4250 rotor to pellet cell fragments and other debris. The supernatant was transferred to a 38 ml ultracentrifuge tube (BD Biosciences, USA, Prod. No. 344058). The tubes were centrifuged at 120,000 × g (RCF AVG, 31300 rpm) for 2 h 40 min at 20 °C, using a SW32ti rotor. The supernatant was removed and the EV pellet was resuspended in 1 ml residual PBS and transferred to a 1 ml ultracentrifuge tube (BD Biosciences, USA, Prod. No. 343778). The tubes were centrifuged at 120,000 × g (RCF AVG, 51000 rpm) for 50 min at 20 °C, using a MLA130 rotor. The supernatant was removed and the EV pellet was resuspended in 200 µl residual PBS.

Density gradient centrifugation was performed using a modified protocol from Brennan et al. To form the gradient, firstly a homogenous base layer of the gradient (estimated density ~ 1.224 g/ml) was produced by adding 672 µl of a 54% iodixanol-PBS working solution (Axis-Shield, UK) to a 13 ml ultracentrifuge tube (BD Biosciences, USA, Prod. No. 344059), together with 200 µl EVs isolated by ultracentrifugation. Next, 3 ml 1.2 g/ml iodixanol and 3 ml 1.08 g/ml iodixanol were layered successively on top of the vesicle suspension with the remainder of the tube filled with PBS. Centrifugation was performed at 197,120 × g (RCF AVG) for 15 h at 4 °C in a SW41ti rotor (40,000 rpm). Fractions (~ 200 µl) were collected from the top of the tube. 50 µl of each fraction was pipetted into a 96 well plate and absorbance was measured at 340 nm against an iodixanol standard curve to determine the fraction density. The fractions with densities between 1.08 and 1.19 g/ml were combined and diluted to a density < 1.03 g/ml with particle-free PBS and the diluted fractions were centrifuged at 120,000 × g (RCF AVG, 31300 rpm using a SW32ti rotor) for 3 h 15 min at 20 °C. The supernatant was removed and the EV pellets were resuspended in 200 µl residual PBS and stored at -80 °C prior to analysis.

EV quantification and characterisation

EV detection and quantification by flow cytometry

EV quantification was performed on the Beckman Coulter CytoFLEX S Flow Cytometer using a modified protocol from Brennan et al.[52]. Events were gated on the VSSC-width log x VSSC-H log cytogram to remove EV aggregates (singlet gate). A rectangular gate was set on the VSSC-H log x RSSC-H log cytogram containing the 80 nm and 500 nm bead populations (Apogee Flow Systems, UK) and defined as 'PS beads 80 nm–500 nm gate' followed by a "stable time gate" set on the time histogram in order to identify the microparticle region. To avoid swarm effects each was serially diluted from 1:2 to 1:500 to achieve an event count of 5000 events/s and measured with a flow rate of 10 µl/min. The EV count was determined as the events/µl within the microparticle region (Supplemental Fig. S1).

EV marker detection by EV-bead conjugated flow cytometry
EV transmembrane markers CD9, CD63, CD81 and CD147 were detected by EV-Bead Conjugated Flow Cytometry on the Beckman Coulter CytoFLEX LX Flow Cytometer using a modified protocol from Brennan et al.[52]. 1.25×10^7 EVs/test was mixed with 0.1 µl/test aldehyde/sulfate latex beads (4 µm; Thermo Fisher Scientific, Waltham, USA) in 200 µl PBS rotating overnight at 4 °C, with beads without EVs being used as a negative control. The beads were blocked in 1% bovine serum albumin (BSA; Sigma-Aldrich, USA), 1 mM EDTA (Sigma-Aldrich, USA), for 1 h at RT, followed by 100 mM glycine (Sigma-Aldrich, USA) for 30 min at room temperature (RT), and 1/50 FC block (BD Bioscience, USA) for 10 min at RT. The samples were then washed with PBS three times and the beads were resuspended in 1% BSA. The beads were stained with antibodies for 30 min on ice and then washed with PBS three times. Flow cytometry analysis was performed on the Beckman Coulter CytoFLEX LX Flow Cytometer, with the gating of EV-decorated 4 µm diameter beads based on FSC/SSC parameters. MIFLowCyt checklist is added as Supplemental Tables S4–S5.

Transmission electron microscopy (TEM)
TEM grids (formvar carbon coated 200 mesh copper grid) were incubated with 10 µl of EV samples in PBS for 60 min. The grids were rinsed by dipping in PBS 3 times for 2 min and dried by a filter paper. The samples were fixed by adding 2.5% glutaraldehyde (Scharlau, Spain) for 10 min followed by washing the grids in distilled water 5 times for 2 min. 2% uranyl acetate (Sigma-Aldrich, USA) was added onto the grids and incubated for 15 min at room temperature. The grids were rinsed quickly with ice-cold 1.8% methyl cellulose (Sigma-Aldrich, USA) and 0.4% uranyl acetate (MC/UA). The samples were embedded by adding MC/UA for 10 min on ice. The grids were air dried at room temperature and examined by TEM (FEI Tecnai™ 120 kV transmission electron microscope, FEI company, USA).

SDS-PAGE and western blot
EV samples were reduced using 4x Laemmli buffer (750 mM Tris-HCl pH 6.8, 5% SDS, 40% glycerol and 80 mM DTT) followed by heating at 95 °C for 5 min. Protein separation was carried out on a 12% SDS-PAGE gel (6% for APOB detection) using a Mini Protean II gel system (Bio-Rad, USA) in Tris-Glycine running buffer at 80 mA for 70 min. Separated proteins were transferred to 0.45 µm PVDF membrane (Merck Millipore, Ireland) using a mini-Protean II blotting system (Bio-Rad, USA) at 110 V constant voltage for 70 min. The membranes were blocked for 1 h at RT in 1X TBS containing 5% (w/v) BSA. Proteins were detected by incubation with primary antibodies in blocking solution overnight at 4 °C. Following three 5 min washes of TBS with 0.1% Tween-20 (TBS-T), membranes were incubated in the appropriate dilution of IRDye800-conjugated goat anti-rabbit IgG and IRDye680-conjugated goat anti-mouse IgG secondary antibodies (LI-COR Biosciences, USA) diluted in 5% blocking solution for 1 h at RT. The blots were then washed six times, alternating between TBS and TBST. Proteins were visualized by scanning the membrane on an Odyssey Infrared Imaging System (LI-COR Biosciences, USA) with both 700- and 800-nm channels.

Mass spectrometry analysis

EV sample preparation
2×10^8 MBS EVs were lysed in ice cold 8 M Urea/50 mM Tris HCL with phosphatase and protease inhibitors (Abcam, AB20111, UK). The EV lysates were reduced and alkylated using dithiothreitol (8 mM final concentration) and iodoacetamide (20 mM final concentration). Then, samples were diluted to 1 M urea using 50 mM Tris-HCl and digestion was continued overnight by the addition of sequencing grade modified trypsin (Promega, Madison, WI, USA, 1:50 trypsin to protein ratio). Following trypsin digestion, the samples were cleaned using Pierce C18 Spin Columns (89870, Thermo Fisher Scientific, USA).

Mass spectrometry analysis
Each sample analysed in duplicate on a Bruker timsTof Pro mass spectrometer connected to an Evosep One liquid chromatography system (Bruker, Denmark). Tryptic peptides were resuspended in 0.1% formic acid and each sample was loaded onto an Evosep tip. The Evosep tips were placed in position on the Evosep One, in a 96-tip box. The autosampler is configured to pick up each tip, elute and separate the peptides using a set chromatography method (30 samples a day). Each sample was eluted from its Evotip onto a 15 cm, 150 µm i.d. analytical column packed with 1.9 µm C18 AQ reverse phase media (V1106 Analytical Column NT—30 samples/day, Evosep, Denmark). Peptides were delivered to the analytical column in buffer a (lcms grade water/0.1% formic acid) and were separated with an increasing buffer B gradient (lcms grade acetonitrile/0.1% formic acid) over 44 min a flow rate of 0.5 µL/min[54]. The mass spectrometer was operated in positive ion mode, with a capillary voltage of 1500 V, dry gas flow of 3 l/min and a dry temperature of 180 °C. All data was acquired with the instrument operating in trapped ion mobility spectrometry (TIMS) mode. Trapped ions were selected for ms/ms using parallel accumulation serial fragmentation (PASEF). A scan range of (100–1700 m/z) was performed at a rate of 5 PASEF MS/MS frames to 1 MS scan with a cycle time of 1.03 s.

Validation of proteomics by Western blot data was previously described[55].

Data analysis
The raw data was searched against the Homo sapiens subset of the UniProt/Swiss-Prot Reviewed FASTA sequence using the search engine MaxQuant (release 2.0.1.0) using specific parameters for trapped ion mobility spectra data dependent acquisition (TIMS DDA). Each peptide used for protein identification met specific MaxQuant parameters. Specifically, only peptide scores that corresponded to a false discovery rate (FDR) of 0.01 were accepted from the MaxQuant database search. The normalised protein intensity of each identified protein was used for label free quantitation (LFQ). Protein was counted as detected if it was counted in more than 60%

of samples in at least one group. Proteins with $p < 0.05$ and fold change of ≤ 0.666 or ≥ 1.5 were selected as significant between F and IF groups.

Venn diagrams were created using Jvenn[56], and heatmaps were created using Morpheus[57], Volcano plots and PCA and were performed using SRPLOT software[58]. GO and Reactome pathway analyses were performed using DAVID 2021[59], $p < 0.05$ was used as threshold. Identification of outliers and AUC curves were made using Metaboanalyst 4.0[60].

Statistical analysis

Statistical analysis was performed using GraphPad PRISM8 software. Differences were considered statistically significant if p value was less than 0.05.

Data availability

The authors confirm that the data supporting the findings of this study can be obtained on reasonable request from Eiva Bernotiene (eiva.bernotiene@imcentras.lt).

Received: 4 November 2024; Accepted: 24 March 2025
Published online: 08 April 2025

References

1. WHO. 1 in 6 people globally affected by infertility: WHO. https://www.who.int/news/item/04-04-2023-1-in-6-people-globally-affected-by-infertility (2023).
2. Sadeghi, M. R. Unexplained infertility, the controversial matter in management of infertile couples. *J. Reprod. Infertil.* **16**, 1–2 (2015).
3. Ortac, M. S. et al. Evaluation of growth hormone deficiency in women with unexplained infertility. *Growth Hormon. IGF Res.* **74**, 101571. https://doi.org/10.1016/j.ghir.2024.101571 (2024).
4. Qu, T. et al. Predictive serum markers for unexplained infertility in child-bearing aged women. *Am. J. Reprod. Immunol.* https://doi.org/10.1111/aji.13194 (2020).
5. Taşkan, T., Turan, T., İltemir Duvan, Z. C. & Gönenç, A. Effect of Fetuin-A and oxidative stress on the occurrence of unexplained infertility. *Turk. J. Obstet. Gynecol.* **20**, 113–119. https://doi.org/10.4274/tjod.galenos.2023.87936 (2023).
6. Fox, C. W. et al. Unexplained recurrent pregnancy loss and unexplained infertility: Twins in disguise. *Hum. Reprod. Open* hoz021. https://doi.org/10.1093/hropen/hoz021 (2020).
7. Wang, L., Lv, S., Mao, W., Pei, M. & Yang, X. Assessment of endometrial receptivity during implantation window in women with unexplained infertility. *Gynecol. Endocrinol.* **36**, 917–921. https://doi.org/10.1080/09513590.2020.1727433 (2020).
8. Gu, J. et al. The effect of chronic endometritis and treatment on patients with unexplained infertility. *BMC Womens Health* **23**, 345. https://doi.org/10.1186/s12905-023-02499-6 (2023).
9. Porpodis, K. et al. Eosinophilic asthma, phenotypes-endotypes and current biomarkers of choice. *J. Pers. Med.* **12**, 1093 (2022).
10. Singh, M., Acharya, N., Shukla, S., Shrivastava, D. & Sharma, G. Comparative study of endometrial & subendometrial angiogenesis in unexplained infertile versus normal fertile women. *Indian J. Med. Res.* **154**, 99–107. https://doi.org/10.4103/ijmr.IJMR_2331_18 (2021).
11. Oger, P. et al. Higher interleukin-18 and mannose-binding lectin are present in uterine lumen of patients with unexplained infertility. *Reprod. Biomed. Online* **19**, 591–598. https://doi.org/10.1016/j.rbmo.2009.05.011 (2009).
12. Ergüven, M., Kahraman, S., Pirkevi, C. & İrez, T. Midkine can not be accepted as a new biomarker for unexplained female infertility. *Turk. J. Biochem.* **48**, 698–708. https://doi.org/10.1515/tjb-2023-0055 (2024).
13. Naseri, S., Lerma, K. & Blumenthal, P. D. Comparative assessment of serum versus menstrual blood for diagnostic purposes. *Obstet. Gynecol.* **133**, 34S. https://doi.org/10.1097/01.AOG.0000559200.04191.a1 (2019).
14. Yang, H., Zhou, B., Prinz, M. & Siegel, D. Proteomic analysis of menstrual blood. *Mol. Cell. Proteom.* **11**, 1024–1035. https://doi.org/10.1074/mcp.M112.018390 (2012).
15. Tindal, K. et al. The composition of menstrual fluid, its applications, and recent advances to understand the endometrial environment: A narrative review. *FS Rev.* **5**, 100075. https://doi.org/10.1016/j.xfnr.2024.100075 (2024).
16. Tang, L. J. et al. Proteomic analysis of human Cervical-Vaginal fluids. *J. Proteome Res.* **6**, 2874–2883. https://doi.org/10.1021/pr0700899 (2007).
17. Van Der Molen, R. G. et al. Menstrual blood closely resembles the uterine immune micro-environment and is clearly distinct from peripheral blood. *Hum. Reprod.* **29**, 303–314. https://doi.org/10.1093/humrep/det398 (2014).
18. Marron, K. & Harrity, C. Potential utility of a non-invasive menstrual blood immunophenotype analysis in reproductive medicine. *Reprod. Fertil.* **3**, 255–261. https://doi.org/10.1530/raf-22-0047 (2022).
19. Hosseini, S. et al. Menstrual blood contains immune cells with inflammatory and anti-inflammatory properties. *J. Obstet. Gynaecol. Res.* **41**, 1803–1812. https://doi.org/10.1111/jog.12801 (2015).
20. Ivarsson, M. A. et al. Composition and dynamics of the uterine NK cell KIR repertoire in menstrual blood. *Mucosal Immunol.* **10**, 322–331. https://doi.org/10.1038/mi.2016.50 (2017).
21. Crona Guterstam, Y. et al. The cytokine profile of menstrual blood. *Acta Obstet. Gynecol. Scand.* **100**, 339–346. https://doi.org/10.1111/aogs.13990 (2021).
22. Naseri, S. et al. Concordance of hemoglobin A1c and reproductive hormone levels in menstrual and venous blood. *FS Rep.* **5**, 33–39. https://doi.org/10.1016/j.xfre.2023.11.009 (2024).
23. Zhou, J. P. et al. Reproductive hormones in menstrual blood. *J. Clin. Endocrinol. Metab.* **69**, 338–342. https://doi.org/10.1210/jcem-69-2-338 (1989).
24. Naseri, S., Brewster, R. C. L. & Blumenthal, P. D. Novel use of menstrual blood for monitoring glycaemic control in patients with diabetes: a proof-of-concept study. *BMJ Sex. Reprod. Health* **48**, 123–127. https://doi.org/10.1136/bmjsrh-2021-201211 (2022).
25. Wong, S. C. C., Au, T. C. C., Chan, S. C. S., Ng, L. P. W. & Tsang, H. F. Menstrual blood human papillomavirus DNA and TAP1 gene polymorphisms as potential biomarkers for screening and monitoring of cervical squamous intraepithelial lesion. *J. Infect. Dis.* **218**, 1739–1745. https://doi.org/10.1093/infdis/jiy369 (2018).
26. Brulport, A. et al. An integrated multi-tissue approach for endometriosis candidate biomarkers: A systematic review. *Reprod. Biol. Endocrinol.* **22**, 21. https://doi.org/10.1186/s12958-023-01181-8 (2024).
27. Dosnon, L., Rduch, T., Meyer, C. & Herrmann, I. K. A Wearable in-pad diagnostic for the detection of disease biomarkers in menstruation blood. *medRxiv*. https://doi.org/10.1101/2024.03.22.24304704 (2024).
28. Palviainen, M. et al. Extracellular vesicles from human plasma and serum are carriers of extravesicular cargo—Implications for biomarker discovery. *PLOS ONE.* **15**, e0236439. https://doi.org/10.1371/journal.pone.0236439 (2020).

29. Es-Haghi, M. et al. Specific trophoblast transcripts transferred by extracellular vesicles affect gene expression in endometrial epithelial cells and May have a role in embryo-maternal crosstalk. *Cell. Commun. Signal.* https://doi.org/10.1186/s12964-019-0448-x (2019).
30. Godakumara, K. et al. Trophoblast derived extracellular vesicles specifically alter the transcriptome of endometrial cells and may constitute a critical component of embryo-maternal communication. *Reprod. Biol. Endocrinol.* https://doi.org/10.1186/s12958-021-00801-5 (2021).
31. Rai, A. et al. Proteomic profiling of human uterine extracellular vesicles reveal dynamic regulation of key players of embryo implantation and fertility during menstrual cycle. *Proteomics* **21**, 2000211. https://doi.org/10.1002/pmic.202000211 (2021).
32. Gardner, D. K. et al. Prospective randomized multicentre comparison on sibling oocytes comparing G-Series media system with antioxidants versus standard G-Series media system. *Reprod. Biomed. Online*. **40**, 637–644. https://doi.org/10.1016/j.rbmo.2020.01.026 (2020).
33. Greening, D. W., Nguyen, H. P., Elgass, K., Simpson, R. J. & Salamonsen, L. A. Human endometrial exosomes contain Hormone-Specific cargo modulating trophoblast adhesive capacity: Insights into endometrial-Embryo interactions. *Biol. Reprod.* **94**, 38. https://doi.org/10.1095/biolreprod.115.134890 (2016).
34. Evans, J. et al. Human endometrial extracellular vesicles functionally prepare human trophectoderm model for implantation: Understanding bidirectional Maternal-Embryo communication. *Proteomics* **19**, e1800423. https://doi.org/10.1002/pmic.201800423 (2019).
35. Hart, A. R. et al. The extracellular vesicles proteome of endometrial cells simulating the receptive menstrual phase differs from that of endometrial cells simulating the non-receptive menstrual phase. *Biomolecules*. https://doi.org/10.3390/biom13020279 (2023).
36. Kusama, K. et al. Intrauterine exosomes are required for bovine conceptus implantation. *Biochem. Biophys. Res. Commun.* **495**, 1370–1375. https://doi.org/10.1016/j.bbrc.2017.11.176 (2018).
37. Riou, C. et al. Avian uterine fluid proteome: Exosomes and biological processes potentially involved in sperm survival. *Mol. Reprod. Dev.* **87**, 454–470. https://doi.org/10.1002/mrd.23333 (2020).
38. Ferraz, M., Carothers, A., Dahal, R., Noonan, M. J. & Songsasen, N. Oviductal extracellular vesicles interact with the spermatozoon's head and mid-piece and improves its motility and fertilizing ability in the domestic Cat. *Sci. Rep.* **9**, 9484. https://doi.org/10.1038/s41598-019-45857-x (2019).
39. Alcântara-Neto, A. S. et al. Porcine oviductal extracellular vesicles interact with gametes and regulate sperm motility and survival. *Theriogenology* **155**, 240–255. https://doi.org/10.1016/j.theriogenology.2020.05.043 (2020).
40. Fereshteh, Z., Bathala, P., Galileo, D. S. & Martin-DeLeon, P. A. Detection of extracellular vesicles in the mouse vaginal fluid: Their delivery of sperm proteins that stimulate capacitation and modulate fertility. *J. Cell. Physiol.* **234**, 12745–12756. https://doi.org/10.1002/jcp.27894 (2019).
41. Al-Dossary, A. A., Strehler, E. E. & Martin-Deleon, P. A. Expression and secretion of plasma membrane Ca^{2+}-ATPase 4a (PMCA4a) during murine estrus: Association with oviductal exosomes and uptake in sperm. *PLoS One* **8**, e80181. https://doi.org/10.1371/journal.pone.0080181 (2013).
42. Schuh, K. et al. Plasma membrane Ca^{2+} ATPase 4 is required for sperm motility and male fertility. *J. Biol. Chem.* **279**, 28220–28226. https://doi.org/10.1074/jbc.M312599200 (2004).
43. Nazri, H. M. et al. Characterization of exosomes in peritoneal fluid of endometriosis patients. *Fertil. Steril.* **113**, 364–373e362. https://doi.org/10.1016/j.fertnstert.2019.09.032 (2020).
44. Welsh, J. A. et al. Minimal information for studies of extracellular vesicles (MISEV2023): From basic to advanced approaches. *J. Extracell. Vesicles*. https://doi.org/10.1002/jev2.12404 (2024).
45. Sohn, J. O. et al. Comparison of extracellular matrix proteins expressed on stromal cells derived from human endometrium with and without spontaneous abortion. *Clin. Exp. Obstet. Gynecol.* **48**, 270. https://doi.org/10.31083/j.ceog.2021.02.2314 (2021).
46. Wróbel, M. et al. Evaluation of proteasome and Immunoproteasome levels in plasma and peritoneal fluid in patients with endometriosis. *Int. J. Mol. Sci.* **24**, 14363. https://doi.org/10.3390/ijms241814363 (2023).
47. Cho, Y. J., Lee, J. E., Park, M. J., O'Malley, B. W. & Han, S. J. Bufalin suppresses endometriosis progression by inducing pyroptosis and apoptosis. *J. Endocrinol.* **237**, 255–269. https://doi.org/10.1530/joe-17-0700 (2018).
48. Chitti, S. V. et al. Vesiclepedia 2024: An extracellular vesicles and extracellular particles repository. *Nucleic Acids Res.* **52**, D1694–D1698. https://doi.org/10.1093/nar/gkad1007 (2024).
49. Liam-Or, R. et al. Cellular uptake and in vivo distribution of mesenchymal-stem-cell-derived extracellular vesicles are protein Corona dependent. *Nat. Nanotechnol.* **19**, 846–855. https://doi.org/10.1038/s41565-023-01585-y (2024).
50. Zheng, S. H. et al. Antioxidant vitamins supplementation reduce endometriosis related pelvic pain in humans: A systematic review and meta-analysis. *Reprod. Biol. Endocrinol.* https://doi.org/10.1186/s12958-023-01126-1 (2023).
51. O'Connor, B. B., Pope, B. D., Peters, M. M., Ris-Stalpers, C. & Parker, K. K. The role of extracellular matrix in normal and pathological pregnancy: Future applications of microphysiological systems in reproductive medicine. *Exp. Biol. Med.* **245**, 1163–1174. https://doi.org/10.1177/1535370220938741 (2020).
52. Brennan, K. et al. Extracellular vesicles isolated from plasma of multiple myeloma patients treated with daratumumab express CD38, PD-L1, and the complement inhibitory proteins CD55 and CD59. *Cells* **11**, 3365. https://doi.org/10.3390/cells11213365 (2022).
53. Livshits, M. A. et al. Isolation of exosomes by differential centrifugation: Theoretical analysis of a commonly used protocol. *Sci. Rep.* **5**, 17319. https://doi.org/10.1038/srep17319 (2015).
54. Bache, N. et al. A novel LC system embeds analytes in pre-formed gradients for rapid, ultra-robust proteomics. *Mol. Cell. Proteom.* **17**, 2284–2296. https://doi.org/10.1074/mcp.TIR118.000853 (2018).
55. Vaiciuleviciute, R. et al. Proteomic signature of menstrual blood mesenchymal stromal cells and their extracellular vesicles in women with unexplained infertility. *Reprod. Biomed. Online*. https://doi.org/10.1016/j.rbmo.2025.104980 (2025). **(In press)**
56. Bardou, P., Mariette, J., Escudié, F., Djemiel, C. & Klopp, C. Jvenn: An interactive Venn diagram viewer. *BMC Bioinform.* **15**, 293. https://doi.org/10.1186/1471-2105-15-293 (2014).
57. Morpheus, https://software.broadinstitute.org/morpheus.
58. Yin, Y. et al. SRplot: A free online platform for data visualization and graphing. *Plos One*. https://doi.org/10.1371/journal.pone.0294236 (2023).
59. Sherman, B. T. et al. DAVID: A web server for functional enrichment analysis and functional annotation of gene lists (2021 update). *Nucleic Acids Res.* **50**, W216–w221. https://doi.org/10.1093/nar/gkac194 (2022).
60. Pang, Z. et al. MetaboAnalyst 6.0: Towards a unified platform for metabolomics data processing, analysis and interpretation. *Nucleic Acids Res.* **52**, W398–W406. https://doi.org/10.1093/nar/gkae253 (2024).

Acknowledgements

This work was funded through European Regional Development Fund activity "Experiment", Project No. 13.1.1-LVPA-K-856-01-0011 "Development of new technology for diagnostics of infertility" led by Ltd Nanodiagnostika. The research was supported by UCD Equip Funding Programme (ref 2021129) and Science Foundation Ireland Research Infrastructure Programme (ref 21/RI/9718); UCD Conway-CEPHR Advanced Cytometry Unit.

Author contributions

K.B.: Formal analysis, Investigation, Writing - Original Draft, R.V.: Formal analysis, Investigation, Writing - Original Draft, Visualization, I.U.: Formal analysis, Investigation, Writing - Original Draft, J.P.: Investigation, L.P.: Resources, Project administration, Funding acquisition, Z.K.: Resources, E.B.: Conceptualization, Methodology, Data Curation, Writing - Review & Editing, Supervision, M.M.M.: Conceptualization, Methodology, Writing - Review & Editing, Supervision.

Declarations

Competing interests

The authors declare no competing interests.

Ethics approval

This study was approved by Vilnius Regional Committee for Biomedical Research Ethics (approval No. 158200-14-741-257 and its addition, no. 158200-741-PP2-34). All participants provided written informed consent prior to enrolment in the study.

Additional information

Supplementary Information The online version contains supplementary material available at https://doi.org/10.1038/s41598-025-95818-w.

Correspondence and requests for materials should be addressed to M.M.M.G.

Reprints and permissions information is available at www.nature.com/reprints.

Publisher's note Springer Nature remains neutral with regard to jurisdictional claims in published maps and institutional affiliations.

Open Access This article is licensed under a Creative Commons Attribution-NonCommercial-NoDerivatives 4.0 International License, which permits any non-commercial use, sharing, distribution and reproduction in any medium or format, as long as you give appropriate credit to the original author(s) and the source, provide a link to the Creative Commons licence, and indicate if you modified the licensed material. You do not have permission under this licence to share adapted material derived from this article or parts of it. The images or other third party material in this article are included in the article's Creative Commons licence, unless indicated otherwise in a credit line to the material. If material is not included in the article's Creative Commons licence and your intended use is not permitted by statutory regulation or exceeds the permitted use, you will need to obtain permission directly from the copyright holder. To view a copy of this licence, visit http://creativecommons.org/licenses/by-nc-nd/4.0/.

© The Author(s) 2025